

# The Use of Hardening Soil Model with Small-Strain Stiffness for Serviceability Limit State Analyses of GRE Structures

## 1) Herold, Andreas

IBH Herold & Partner Ingenieure, Weimar, Germany

## 2) von Wolfersdorff, Peter-Andreas

BAUGRUND DRESDEN Ingenieurgesellschaft mbH, Dresden, Germany

*Abstract:* Advanced constitutive models accounting for increased stiffness of soils at small strains offer a significant improvement in accuracy when undertaking soil-structure interaction modelling and for subsequent reliable displacement prediction at working load conditions. Current paper describes the use of the Hardening Soil Model with Small-Strain Stiffness (HSsmall) for evaluation of the Serviceability Limit State (USL) of Geosynthetic Reinforced Earth (GRE) structures. Emphasis is put on the practical use rather than on the mathematical description. The laboratory tests for determination of necessary soil mechanical parameters are explained. Further, deformation measurements of MSE-Walls in large scale are used for validation of numerical calculation results. It is shown that the calculated results are in good agreement with expected deformations. In addition, it is shown that HSsmall constitutive model can also be utilized for dynamic problems.

### 1. Introduction

In January 2005 the German standard for Geotechnical design, entitled DIN 1054:2005-01, was published. It regulates fundamental questions of geotechnical and foundation engineering stability analyses under the partial safety concept. The following limit states are differentiated using the new safety factor approach:

- Ultimate Limit State (ULS)
- Serviceability Limit State (USL)

The ULS is a condition of the structure which, if exceeded, immediately leads to a mathematical collapse or other form of failure. The SLS is a condition of the structure which, if exceeded, no

longer fulfils the conditions specified for its use, without a loss of bearing capacity. For geotechnical constructions, the SLS includes the serviceability of the earthwork and neighbouring buildings or structures. In this context, the amendment of the German recommendation for geosynthetic reinforced earth structures, entitled EBGEO (2009-draft) [1], regulates in particular the SLS calculations of Geosynthetic Reinforced Earth (GRE) structures. In compliance with the principles and rules of DIN 1054:2005-01, the limit state design requirements are based on the classification of the structure into particular Geotechnical Categories 1, 2 and 3, according to the complexity of the structure, of the ground conditions and the

loading, and the level of risk that is acceptable for the purpose of the structure. Calculation of expected deformations of GRE structures is difficult due to the composite construction method, composed of both construction materials soil and geosynthetic. In particular the complex soil-structure interaction can be approximated limited with existing constitute laws. This very issue is addressed in [2]. The obvious question which the practical engineer, will ask is: “How to calculate the expected deformations?” and/or “How to check the relevant serviceability requirements?”. A constitutive law describing the soil-geosynthetics interaction behaviour as a composite material is presented, as a first approach, in [3]. The research and development in the field of constitutive models for individual construction materials is well advanced, so that for practical application various constitutive models are available. They allow an easy determination of material parameters, and deliver realistic results. Most commonly used constitutive laws are the Mohr-Coulomb model (MC) and the Hardening-Soil model (HS). The simplicity of the MC-model allows a fast and simple application, but does not account for typical characteristic of soils, such as the stress-dependant stiffness behaviour and irreversible strains due to primary isotropic compression. These essential aspects are covered by the more advanced HS-model, an elastoplastic model with isotropic hardening. Recently, the HS-model was extended with small-strain stiffness (HSsmall). The HSsmall model is a modification of the HS-model that accounts for the increased stiffness of soils at small strains. At low strain levels most soils exhibit a higher stiffness than at engineering strain levels, this stiffness varies non-linearly with strain. HSsmall model is suitable for the analysis of both static and dynamic tasks. The HSsmall

model has been implemented in PLAXIS (v.9) [4], a commercially available software.

### 1.1. HSsmall-Model

The original Hardening Soil (HS) model assumes elastic material behaviour during unloading and reloading. However, the strain range in which soils can be considered truly elastic, i.e. where they recover from applied straining almost completely, is very small. With increasing strain amplitude, soil stiffness decays nonlinearly. Figure 1 gives an example of such a stiffness reduction curve. It shows the characteristic stiffness-strain behaviour of soil with typical strain ranges for laboratory tests and structures.

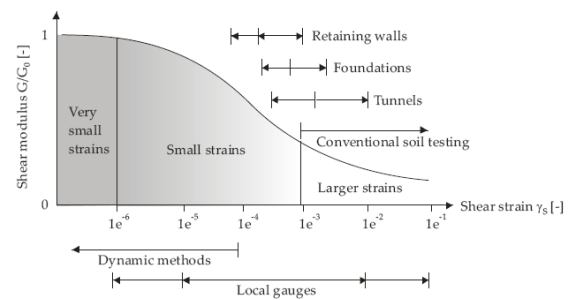


Figure 1: Characteristic stiffness-strain behaviour of soil with typical strain ranges for laboratory tests and structures according to [4]

One feature of soil behaviour that was still missing in the HS-model is the high stiffness at small strain levels ( $< 10^{-5}$ ). Even in applications that are dominated by ‘engineering strain levels’ ( $> 10^{-3}$ ) small-strain stiffness can play an important role. It is generally known that conventional models over-predict heave in excavation problems. These models also over-predict the width and under-predict the gradient of the settlement trough behind excavations and above tunnels. Small-strain stiffness can improve this. Moreover small-strain stiffness can be used to model the effect of hysteresis and hysteretic damping in applications involving cyclic loading and dynamic behaviour [4].

The HSsmall model is based on the Hardening Soil (HS) model and uses almost entirely the same parameters. In fact, only two additional parameters are needed to describe the stiffness behaviour at small strains. These are

- the initial or very small-strain shear modulus  $G_0^{\text{ref}}$ , and
- the shear strain level  $\gamma_{0,7}$  at which the secant shear modulus  $G$  is reduced to 70 % of  $G_0^{\text{re}}$ .

The following equation according to [4] and [6] shows the corresponding relationship between  $G_0^{\text{ref}}$  und  $\gamma_{0,7}$ .

$$\frac{G_s}{G_0} = \frac{1}{1 + \frac{3}{7} \cdot \left| \frac{\gamma}{\gamma_{0,7}} \right|}$$

The advanced features of the HSsmall model are most apparent in working load conditions. Here, the model gives more reliable displacements than the HS-model. When used in dynamic applications, the HSsmall model also introduces hysteric material damping. Thus, this advanced constitutive model is specially suited for analysis of ductile structures (e.g. GRE), both for static and dynamic applications. The material parameters of the HSsmall model can be obtained by conducting classical laboratory tests, i.e. triaxial tests (see Figure 2) and resonant-column tests without special instrumentation.

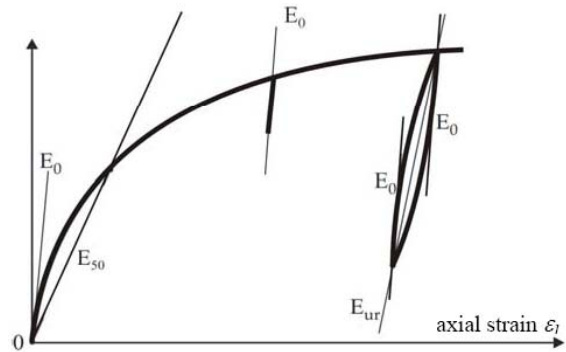


Figure 2: Model parameters for HSsmall-Model according to [4]

In soil dynamics, small-strain stiffness has been a well known phenomenon for a long time. In static analysis, the findings from soil dynamics have long been considered not to be applicable. Seeming differences between static and dynamic soil stiffness have been attributed to the nature of loading (e.g. inertia forces and strain rate effects) rather than to the magnitude of applied strain which is generally small in dynamic conditions (earthquakes excluded). As inertia forces and strain rate have only little influence on the initial soil stiffness, dynamic soil stiffness and small-strain stiffness can in fact be considered as synonyms.

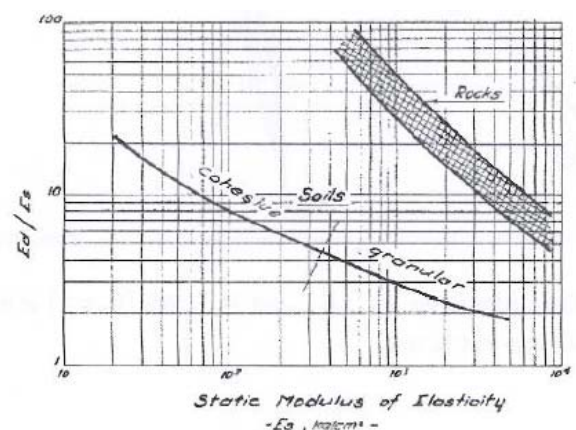


Figure 3: Static-dynamic Modulus of Elasticity according to [6]

The advantage of using the HSsmall in combination with dynamic calculations becomes obvious. The well known phenomenon of small-

strain stiffness in soil dynamics (as described in [7] and [8] and depicted in Figure 3) can be utilized in numerical calculations.

### 1.2. Laboratory Testing

Extensive laboratory tests have been performed on two different sandy soils. These two soils were used for the large scale experiments (“Riga” and “Cottbus”) as described in Section 2. The sands have been tested to determine the necessary material parameters for the HSsmall model. Table 1 summarizes the identified properties for the sand used in the large scale experiment “Cottbus”.

Table 1: HSs model parameters, experiment “Cottbus”

| Parameter:       | Dimension:               | Value:               | Legend:   |
|------------------|--------------------------|----------------------|---|
| $\rho$           | $[\text{kg}/\text{m}^3]$ | 1840                 | dry density   |
| $\rho_d$         | $[\text{kg}/\text{m}^3]$ | 1763                 | dry density in test   |
| $D_{50}$         | [1]                      | ~ 1,00               | Compression ratio   |
| $w$              | [1]                      | 0,043                | moisture content  |
| $\phi'$          | [°]                      | 38,3                 | Friction angle  |
| $c'$             | $[\text{kN}/\text{m}^2]$ | 1,0                  | Cohesion  |
| $\psi$           | [°]                      | 6,02                 | Dilatance angle   |
| $p^{ref}$        | $[\text{kN}/\text{m}^2]$ | 100,00               | Reference voltage   |
| $m$              | [1]                      | 0,88                 | Power   |
| $E_{0ed}^{ref}$  | $[\text{kN}/\text{m}^2]$ | 79.400,00            | Reference value of the stiffness modulus  |
| $E_{50}^{ref}$   | $[\text{kN}/\text{m}^2]$ | 53.900,00            | Reference value of the elastic modulus with half of the ultimate shear stress           |
| $E_{var}^{ref}$  | $[\text{kN}/\text{m}^2]$ | 145.900,00           | Reference value of the elastic modulus during discharge and reload                      |
| $\nu_{gr}$       | [1]                      | 0,28                 | Poisson's ratio   |
| $R_0$            | [1]                      | 0,84                 | stress ratio  |
| $G_0^{ref}$      | $[\text{kN}/\text{m}^2]$ | 98.400,00            | Reference value of the shear modulus at small stretches                                 |
| $\epsilon_{0,2}$ | [1]                      | $6,89 \cdot 10^{-4}$ | Reference value of shear strain with approximately 72.2% reduction of the shear modulus |

Figure 4 shows the result (deviatoric stresses vs. vertical deformation) of a triaxial test carried out at a reference stress of  $100 \text{ kN}/\text{m}^2$ . The test was conducted with a single discharge at approximately 1% vertical deformation.

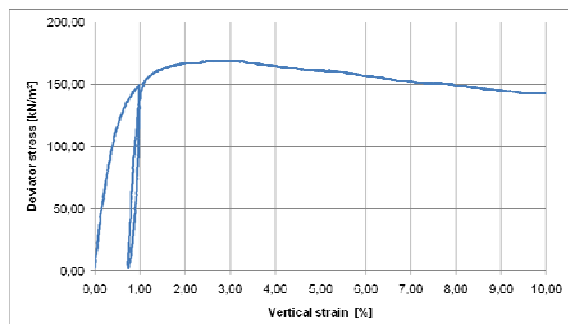


Figure 4: Result of a triaxial test

In addition, resonant column tests have been performed for evaluating the strain-dependent modulus. Due to the lack of space a presentation of the resonant-column test results is waived. With the determined HSsmall parameters the large scale experiments were back-calculated and verified.

## 2. Large Scale Experiment

Two large scale experiments were conducted at static and dynamic loading conditions. Both experiments were extensively instrumented. Through this a comparison of measurement results and the results of numerical calculations were given. In the following the experimental setup and procedure is described in detail.

### 2.1. Large Scale Experiment “Riga”

In 2008, a large scale experiment was carried out at a GRE structure (6 m high) in Riga. The boundary conditions, experimental setup and procedure are described in detail in [9]. Figure 5 shows the GRE arrangement, the measuring system and the loading condition.

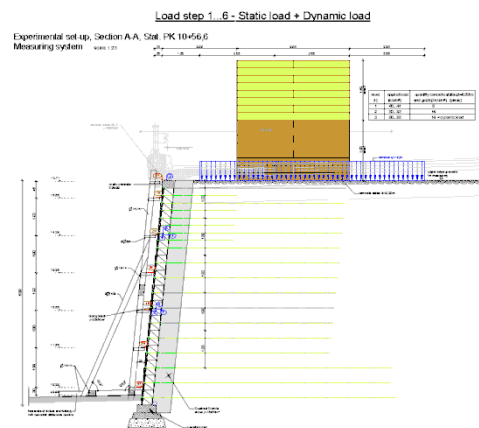


Figure 5: Large scale experiment “Riga”: Experimental setup and measuring system

The experimental procedure utilizes dead loads. The dead load was gradually applied via concrete plates.

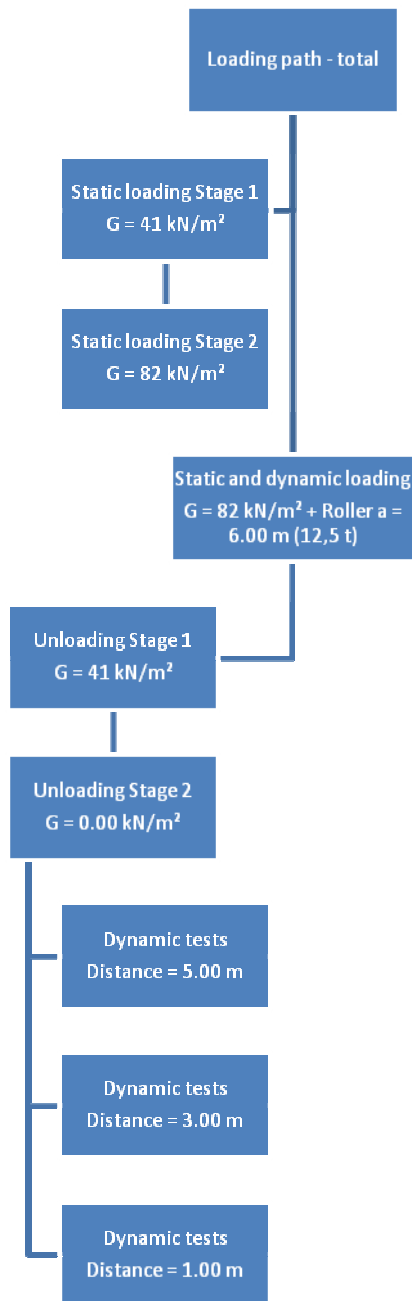


Figure 6: Large scale experiment "Riga": Loading history

As regular loads from heavy trucks should be simulated, twice the prognosticated distributed static load was applied – being on the safe side. The horizontal and vertical deformations at the front wall were monitored over the entire test period of three days. During the dynamic loading phases using a 12,5 t vibratory roller vibration velocity measurements were executed. The static load was applied in several steps and was completely removed at the end of the

experiment. Figure 6 depicts the loading history. The entire experimental setup including the static loading configuration is depicted in Figure 7.



Figure 7: Large scale experiment "Riga"

## 2.2. Large Scale Experiment "Cottbus"

Two large scale experiments with different front systems were planned and performed in the framework of a cooperative research at the BTU Cottbus. Hereby the reinforcement type, the spacing, and as well as the static loading were varied.

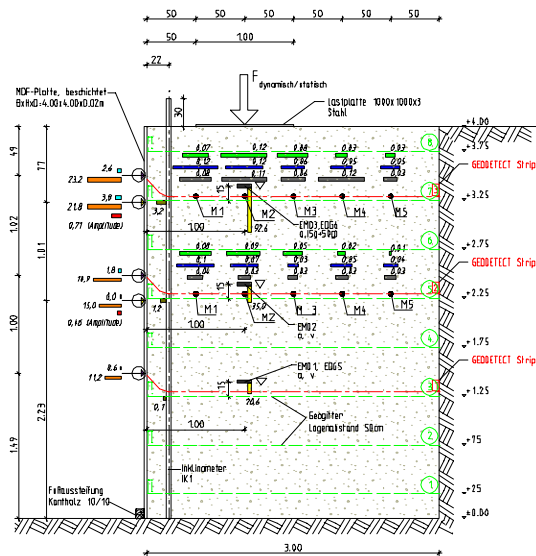


Figure 8: Large scale experiment "Cottbus"; Measuring section



Figure 9: Large scale experiment "Cottbus", Dynamic loading

In addition, different dynamic vibration loading with various frequency and load amplitude were applied. The experiments are described in detail in [10] and [11]. Figure 8 shows the measuring section with corresponding instrumentation. Figure 9 shows the dynamic loading using a heavy vibrating roller.

### 2.3. Comparison of Measurement Results

The objective of the numerical calculations with the finite element software PLAXIS v.9 was to compare the numerical results with the experimental measured values to check the suitability and the quality of the constitutive model used. Figure 10 and Figure 11 show exemplary the results for the experiment "Cottbus". The computational section and the contours of magnitude of horizontal displacements as induced by a static load of 350 kN/m<sup>2</sup> are shown in Figure 10. This model uses the elastic-perfectly plastic Mohr-Coulomb model. A comparison of measured and calculated horizontal displacements at a selected point (h = 3.75 m) is shown in Figure 11. The diagram shows

results from the finite element calculation using the MC-model and the HSsmall model.

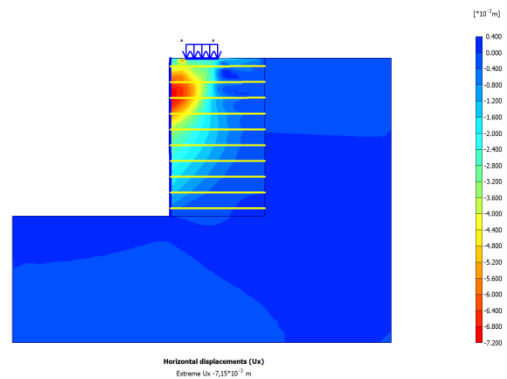


Figure 10: Experiment "Cottbus"; Horizontal displacements, static, 350 kN/m<sup>2</sup>

As it can be seen from Figure 11, the calculated results using HSsmall model almost fit the measured horizontal displacements, both for small and ultimate surcharge load (ranging between 350-400 kN/m<sup>2</sup>).

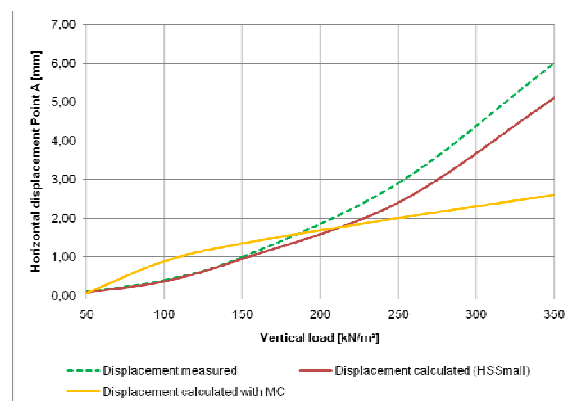


Figure 11: Experiment "Cottbus"; Comparison of vertical and horizontal displacements, static, H = 3,75 m (front)

The calculated results using MC-model deviates clearly from the measured horizontal displacements. At small surcharge loads the MC-model delivers higher displacements than actually measured. At higher surcharge loads the MC-model delivers half the measured displacements.

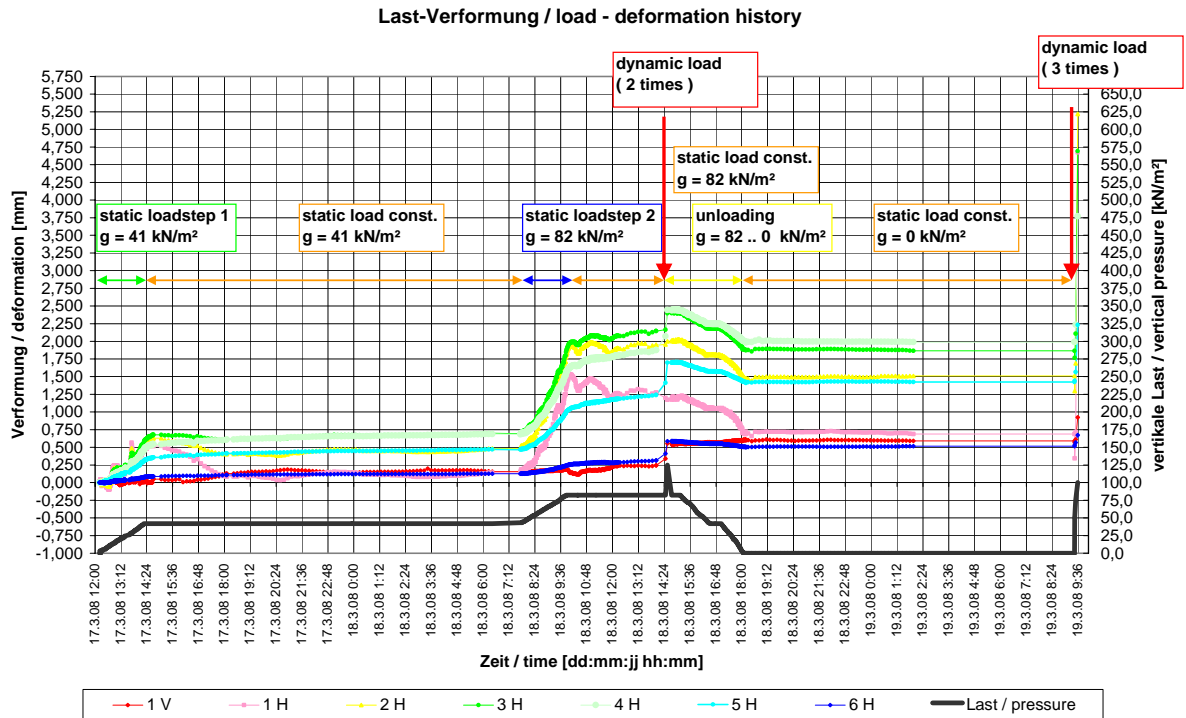


Figure 12: Large scale experiment „Riga“; Load-deformation history of horizontal displacements

This is because the MC-Model does not take the small-strain stiffness in account as shown in Figure 1.

Figure 12 shows the measured horizontal displacements as a function of the time and loading history for the large scale experiment “Riga”. Figure 13 shows finite element model and the computational results at the maximal static loading stage.

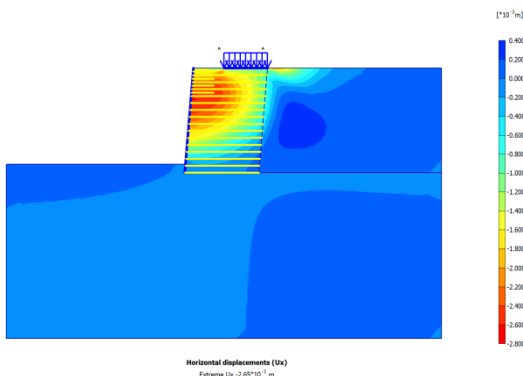


Figure 13: Large scale Experiment „Riga“; Horizontal displacement, static, 82 kN/m²

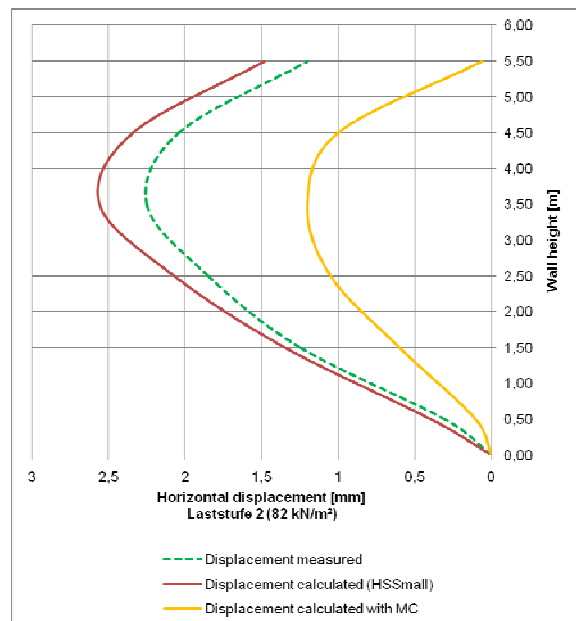


Figure 14: Large scale experiment „Riga“; Comparison of horizontal displacements

Comparisons of measured and calculated horizontal displacements are shown in Figure 14. As it can be seen from the comparison, the aforementioned lack of the MC-model is obvious.

### 3. Conclusions

This paper contains a direct comparison of experimentally measured and numerically calculated results for two GRE structures. The soil was modelled using the simple Mohr-Coulomb (MC) model, the more advanced Hardening Soil model with small-strain stiffness (HSsmall model). It may be concluded from this study:

- HSsmall model is suitable for the analysis of both static and dynamic tasks, and for deformation calculations of GRD structures with non-cohesive soils.
- The calculated results using HSsmall model almost fit the measured displacements, both for static and dynamic load cases.
- The expenses for determination of material parameters for HSsmall model are low compared to increase of the quality of the calculation results.
- A realistic estimation of deformations can be realized by user-friendly software such as PLAXIS v.9 [4], which incorporates advanced constitutive models like HSsmall model.

Overall, it can be concluded that the time required for the pre- and post- processing of engineering practical applications are quite sufficient. The serviceability requirements of DIN 1054:2005-01 and EBGEO [1] can be met.

### 4. References

- [1] EBGEO (2009): German Recommendations for Geosynthetic Reinforced Earth Structures. Draft 02/2009a; German Geotechnical Society (DGGT)  
[www.gb.bv.tum.de/fachsektion/b\\_ak-ak52.htm](http://www.gb.bv.tum.de/fachsektion/b_ak-ak52.htm)
- [2] Herold, A. (2007): 10 Jahre Verformungsbeobachtungen an KBE-Bauwerken – Ist die Dehnsteifigkeit der Geokunststoffe der Schlüssel zur korrekten Prognose des Verformungsverhaltens von KBE-Stützbauwerken?. Geotechnik 29(2007)2, pp. 79-86.
- [3] Ruiken, A.; Ziegler, M. (2009): Untersuchung des Tragkraft-Verformungsverhaltens von geogitterbewehrtem Boden. Geotechnik Sonderheft 2009.
- [4] Plaxis Software Delft (2008): Material Models Manual. Version 9.01, PLAXIS BV, The Netherlands.
- [5] Vucetic, M. (1994): Cyclic Threshold Shear Strains in Soils. ASCE, Journal of Geotechnical Engineering, Vol. 120, 1994, No. 12.
- [6] Santos, J.A.; Correia, A.G. (2001). Reference threshold shear strain of soil application to obtain a unique strain-dependent shear modulus curve for soil. Proc. 15th Int. Conf. on Soil Mechanics and Geotechnical Engineering 2001. Istanbul, Turkey, Vol. 1: pp. 267-270.
- [7] Alpan, I. (1970): The geotechnical properties of soils. Earth-Science Reviews, 6: pp. 5-49.
- [8] Empfehlungen des Arbeitskreises "Baugrunddynamik" (2002): German Geotechnical Society (DGGT).
- [9] Hangen, H.; Herold, A. Et al. (2008): Construction of the bridge approach embankments for Riga's South Bridge: Case study. 11th Baltic Sea Conference Gdansk 2008, Conference Proceedings.
- [10] Klapperich, H.; Herold, A. (2007): Neues rund um's Geogitter. 4. Geokunststoff Kolloquium, Bad Lauterberg.
- [11] Pachomov, D.; Vollmert, L. and Herold, A. (2007): Der Ansatz des horizontalen Erddruckes auf die Front von KBE-Systemen. FS-KGEO 2007, Sonderheft Geotechnik.